Indonesian Journal of Electrical Engineering and Computer Science
Vol. 3, No. 3, September 2016, pp. 646 ~ 654
DOI: 10.11591/ijeecs.v3.i2.pp646-654

An Equivalent Electrode System for Efficient Charging of Filtration Media

Mohamed A. Abouelatta
Shoubra Faculty of Engineering, Benha University, 108 Shoubra St., Cairo, Egypt
E-mail: moh_an1@yahoo.com

Abstract

This paper concerns the influence of moving an auxiliary limiting cylinder in X-Y directions on the electrostatic field and corona onset voltage of the dual electrode system employed in the electrostatic filtration process resulting in a "Tri-electrode" system. The Tri-electrode system is applied in order to control the field around the ionized wire and on the ground plate. Accurate calculation of the electrostatic field is obtained using the charge simulation method coupled with genetic algorithms. The calculated field values are utilized in computing the corona onset voltage of the ionized electrode. Laboratory measurements of the onset voltage of the ionized electrode are applied. It is found that the limiting cylinder controls the onset voltage of the ionized wire such that the ionized wire may be in ionized or non-ionized state without changing the position of the ionized wire itself. The numerical onset voltage values agreed satisfactorily with those measured experimentally.

Keywords*: corona discharge, tri-electrode system, filtration media, electric field*

1. Introduction

Filtration process is implemented in many applications including water purification, beneficiation of minerals, biotechnologies and chemical industries [1, 2]. A filter medium is a pervious and flexible material through which a fluid (liquid, gases) flows through it such that the particles suspended in it is retained [3, 4]. The filters may be natural like cotton, wool or artificial like polyethylene, polyester [1, 2]. So, filtration helps in preventing damage resulting from contamination, as well as in increasing the availability of the system which results in increasing productivity considerably.

Both woven and non-woven materials are employed as fibers media. Needle punching and melt- blowing are the most popular technologies utilized to construct a non-woven media [1, 2]. Needle punching is carried out by squeezing the fibers using two plates, while melt- blowing is performed by puffing the fibers with very hot air and stress them by a drum system. Unpleasant smells may pass through the filter, so the filter media should contain active carbon powder to neutralize these smells [4, 5].

Corona discharges are presently used in electrical charging of filtration media using different electrode configurations like dual electrode system, blade-cylinder electrode, needles-cylinder electrode [6, 7]. The dual electrode system is the most commonly configuration applied in electrostatic charging of dielectric media despite being encountered to mechanical damage [8, 9]. The dual electrode system, figure 1a, is a system comprising an ionizing wire and a non-ionizing metallic cylinder electrode, all at the same potential. The cylinder serves as a metallic support for the ionizing wire as well as its effect on the onset voltage of the wire and corona discharges [8].

The geometrical parameters of such system (h, d) and the applied voltage have a great influence on the filtration process. But actually, a better control over the geometrical parameters is not easy, due to the limited space of dual electrode system. So, the corona onset voltage and the ground current density can not be well controlled. Besides, the discharging zone is one of the major problems facing the designers to control the flow of electric charges produced by the corona discharge and prevent it from flowing to any nearby elements to the ionizing electrode.

To overcome the above control problem, a new proposed Tri-electrode system was suggested to provide a wider control over the corona onset voltage through the insertion of an auxiliary wire in the region between the main ionized wire and the upper metallic cylinder [10].

Received April 2, 2016; Revised July 25, 2016; Accepted August 10, 2016

The new system can be also termed as “switchable dual electrode” system as auxiliary cylinder controls the onset voltage of the ionized wire such that the wire may be in the ionizing state or in non-ionizing state. Another Tri-electrode system was proposed but here an auxiliary cylinder were placed parallel to the ionized wire far away from the metallic cylinder, Figure 2(b), [11]. During the charging process of the filtration media, the auxiliary cylinder increases the electric field on the ground surface and the space charge density but the effect of changing the position of the auxiliary limiting cylinder on the value of the corona onset voltage was not studied which reflects into the stressing of higher applied voltages.

The aim of the present paper is to show the effectiveness of moving the auxiliary limiting cylinder of the Tri-electrode system on the profile of the electrostatic field on the ground and the field modulation on the surface of the ionized wire. The auxiliary cylinder will be allowed to move through the gap along the x-axis as well as the Y-axis. Such arrangement will provide reliability into controlling the electrostatic field not only on the ionized wire surface but also along the ground surface. The arrangement also offers more flexibility, high efficiency and ease of operation in the filtration media. The present work uses the charge simulation method (CSM) coupled with the genetic algorithms (GAs) to model the electrostatic field on the ground and on the surface of the ionized wire. Experiments will be carried out for different ionized wire diameters between 0.25-1 mm to show the effectiveness of the movement of the limiting cylinder in the two -dimensional on the corona onset voltage of the ionized wire.

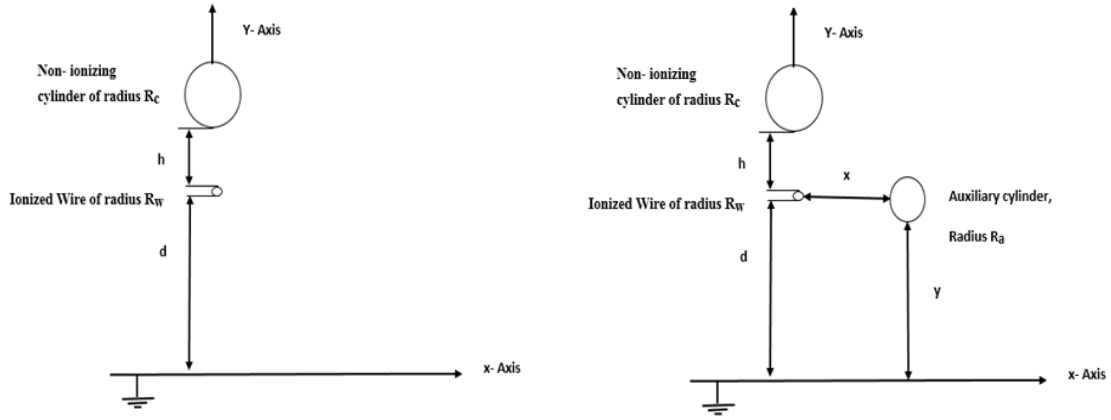

Figure 1. (a) Dual electrode configuration; (b) Tri-electrode configuration

2. Corona Onset and Electric Field Calculation

Neglecting the edge effect of the electrodes, and assuming constant and uniform corona discharge, the space charge free case computation is performed in a two-dimensional domain. Laplace's equation is implemented to compute the space charge- free electric field E as follows:

$$\Delta V=0 \tag{1}$$

Where, V is the electric potential and, the electric field is given by:

$$E = - \nabla V \tag{2}$$

The corona onset electric field E_{on} is computed using peek’s formula [12]:

$$E_{on} = 31\delta\left[1+\frac{0308}{\sqrt{r}}\right] \qquad kV/cm \tag{3}$$

Where, δ is the air density and r is the radius of the wire in cm.

Figure 1(b) shows a Tri-electrode system stressed by a voltage V and positioned in air. The three electrodes have a potential V and the collector plate is grounded. The analysis of space charge- free electric field computation is based on charge simulation method (CSM) integrated with genetic algorithm (GA) [13]. A set of simulating line charges is positioned at the inner surfaces of the stressed electrodes, Figure 2. Equal number of contour points, corresponding to the simulating charges, is selected along these surfaces. Equation (5) is constructed and solved to determine the magnitude of the simulation charges Q:

$$[P]\,[Q] = [V] \tag{4}$$

$$[F_X][Q] = [E_X] \tag{5}$$

$$[F_Y]\,[Q] = [E_Y] \tag{6}$$

Where P is the potential coefficient matrix determined by the location of the charges and the contour points, Q is the unknown charges vector; V is the known potentials vector at the contour points. F_X and F_Y are the electric field intensity coefficients between the simulation charges and the electric field intensity components at the point where this field is calculated. E_X and E_Y are the components of the electric field intensity at the same point.

Eight, fifty and twenty four line charges are placed inside the ionizing wire, the cylindrical electrode and the limiting auxiliary cylinder on hypothetical parallel cylindrical surfaces of diameters $2R_w*K_1$, $2R_c*K_2$ and $2R_a*K_3$ respectively, Figure 2. A range between 0 and 1 is taken for the optimization parameters values K_1, K_2 and K_3. The method of image is applied to model the ground plate. Charge simulation method is coupled with genetic algorithms (GA-CSM), in the MATLAB environment, to determine the optimal values of K_1, K_2 and K_3 based upon the minimization of the accumulated square error (ASE) of the potential values along all the electrodes' surfaces [13]. The objective fitness function, *FF*, is proposed as follows:

$$FF = \sum_{j=1}^{N_h} \left[V - v_j\right]^2 \tag{7}$$

Where, V is the electrode voltage of the three electrodes (1 p.u), v_j is the potential obtained by the CSM at the check point j and N_h is the total number of check points.

Further Details about GA operations and implementations are illustrated in [14-16]. The sequence of the proposed GA-CSM algorithm is as follows:

1. Choose the optimization parameters area.
2. Initial uniform random values for K_1, K_2 and K_3 is created using GA.
3. CSM generates the ASE error for this set of optimization parameters during each call to the CSM routine by GA.
4. Then, the GA will estimate the fitness function and minimize the ASE error by modifying the optimization.
5. Steps 3-4 are repeated for the selected number of generations.

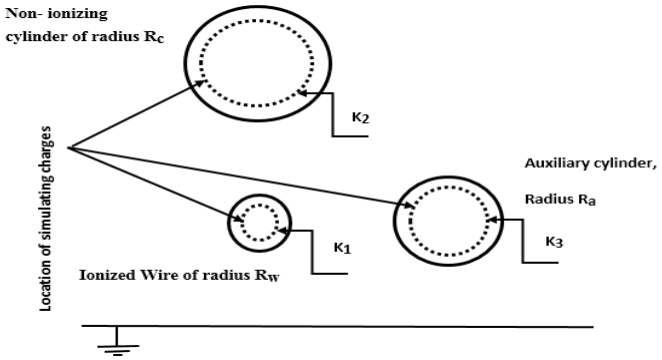

Figure 2. The optimization parameters (K_1, K_2 , K_3) for the arrangement of the simulating charges in the CSM

3. Corona Onset Voltage Measurement

The experimental set-up for the measurement of onset voltage of ionized wire, in the presence of an auxiliary limiting cylinder is presented in Figure 3. The measurements were carried out in atmospheric air. A tungsten wire of radius R_w is placed parallel to and above the ground plate at a distance d equal to 25 mm from the surface of the grounded plate and hanged using a non-ionizing cylinder of circular cross section (radius R_c = 12.5 mm) at a distance h equals to 20 mm above the ionized wire. Both of them are on the same y-axis. The auxiliary limiting cylinder of radius R_a is positioned parallel to the two electrodes at distance, x, from the ionized wire and hanged at distance, y, from the ground plate. A negative high voltage DC source (Hipotronics, Model 800PL-10MA series) has been employed to energize the three stressed electrodse up to 80 kV and 10 mA. The ground plate electrode was (287×144)mm with a rounded edge to avoid the occurrence of coronas at this edge.

The audible corona onset voltage was measured on the surface of the ionized electrode. The applied voltage was increased in a silent laboratory to about 80% of the expected value at a rate of 0.5 kV/sec and thereafter at a rate of about 0.1 kV/sec until it was just possible to hear the flutter sound [17]. Ten measurements were developed to estimate the average of each measuring value. A minimum of one minute was selected for the time interval between two successive applied voltages. The standard deviation of the average values was generally smaller than 1%. The measurements have been prepared in dry air at room temperature (about 20-25º C) and atmospheric pressure.

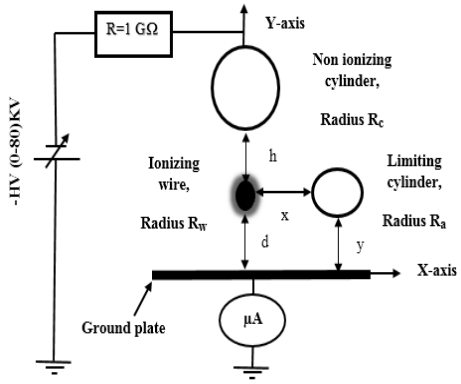

Figure 3. Experimental Setup

4. Results and Analysis

To check the accuracy of the proposed GA-CSM for the Tri-electrode system, the potential at the ionized wire surface is assessed at the check points to check the satisfaction of the boundary condition upon it. The check points are selected midway between the contour points. The percentage ASE and maximum potential error on the surface of the ionized wire for the different simulation results is computed and were not exceeding $2*10^{-5}$% which reflects the validity of the presented algorithm. The percentage potential error at the ionized wire surface for one of these results is plotted in Figure 4.

Also, accurate computation of the electrostatic field using the proposed GA-CSM compared with COMSOL Multiphysics version (4.2a), based on finite element method (FEM) is realized in order to validate the results obtained by such method. Figure 5 represents the variation of electric field on the ground surface for dual and tri-electrode systems using the two methods. A good agreement between the CSM and FEM (COMSOL) was found for the two methods.

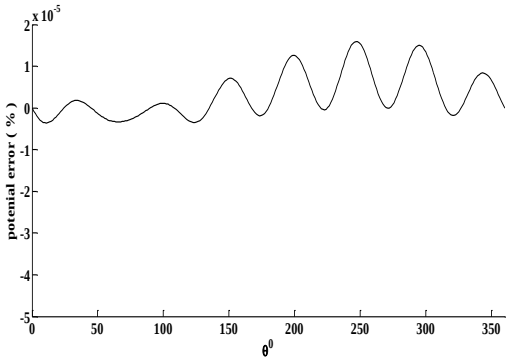

Figure 4. Percentage Potential error at the surface of the ionized wire in Tri-electrode system (V=10kV, $2R_a$=14mm, $2R_w$=0.5mm, $2R_c$=25mm, h=20mm, d=25mm, x=25mm, y=25mm)

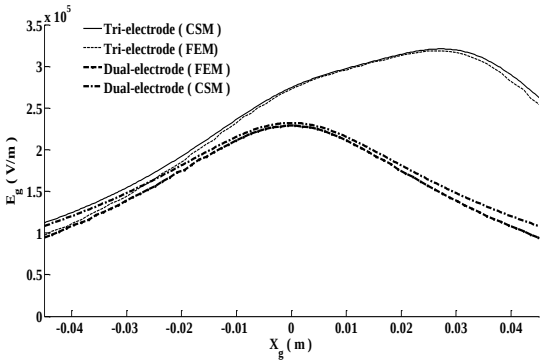

Figure 5. Variation of electrostatic field on the ground plate (V=10kV, $2R_a$=14mm, $2R_w$=0.5mm, $2R_c$=25mm, h=20mm, d=25mm)

The variation of electrostatic field upon the ground plate for dual and tri-electrode systems has been studied in Figure 6(a). A higher asymmetric electric field is realized when the limiting cylinder is attached to the dual electrode system. The electric field at x_g=0 grows by 18.5% by positioning the auxiliary cylinder at (x=25, y= 25) mm from the ionized wire. It is observed that the electric field is higher in the zone where the auxiliary cylinder is located. So, the electrostatic field upon the ground surface can be increased without changing the position of the ionized wire.

Figure 6(b) shows the modulation of electrostatic field at the ionized wire for dual and tri-electrode systems. Due to the presence of limiting cylinder, a lower electric field is realized. The maximum electric field decreases by 15 %. The difference between E_{max} and E_{min} is 19.43% in dual system and 15.35% by positioning the auxiliary cylinder at (x=25, y= 25) mm from the ionized wire. The existence of the extra cylinder increase the non-uniformity around the wire. It must be noticed that the angle at which maximum field occurs on the wire decreases by 7.20° when the limiting cylinder is attached to dual electrode system. So, the electrostatic field at the ionized wire can be controlled without moving the ionized wire.

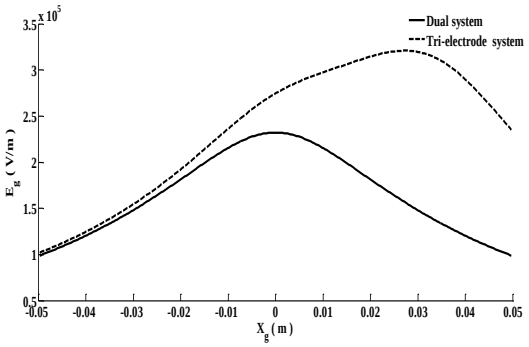

(a) on the ground plate

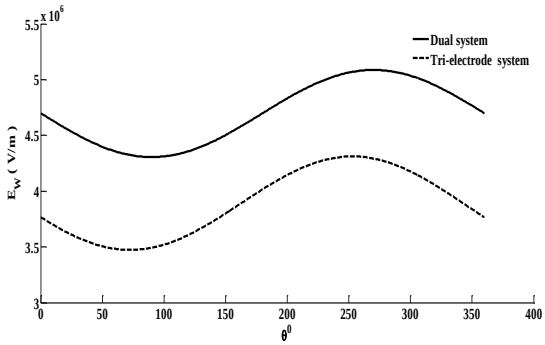

(b) at the ionized wire

Figure 6. Variation of electrostatic field (V=10kV, $2R_a$=14mm, $2R_w$=0.5mm, $2R_c$=25mm, h=20mm, d=25mm, x=25mm,y=25mm)

The computation of the electrostatic field identified that the geometrical parameters of the dual electrode system have a great influence on the filtration efficiency. Depending on the particles to be filtered, the operating conditions are employed to obtain high filtration efficiency. The location of the ionized wire greatly affects the filtration process. So, it must be carefully

located in order to get maximum field strength in the area located between the ionized wire and the ground plate. As the non- ionizing cylinder gets closer to the ionized wire, the corona onset voltage increases results in a lower charge emission [8-9], [19].

Figure 7(a) shows the influence of changing the inter-electrode distance (d) on the shape of the electrostatic field on the ground surface. The maximum electric field on the ground surface increases slightly as the distance (d) decreases. It should be locked out that the region where the limiting cylinder is located is not remarkably changed in contrary to the left zone where there is no limiting cylinder.

The effect of the inter-electrode distance (d) variation on the shape of the electrostatic field upon the ionized wire is expressed in Figure 7(b). The maximum electric field on the wire increases as the distance (d) decreases. The maximum electric field on the wire is decreased by 5.8%, 11.4%,and 15.8% when distance,d, is changed from d=23 to 25, 27 and 29 mm respectively. The variation between E_{max} and E_{min} is 19.3%, 19.4%, 19.6%, 19.7% at d= 23, 25, 27and 29 mm respectively. It is observed that the non-uniformity around the ionized wire is almost stable unlike the dual system when changing the distance (d). But in practical situations, changing distance (d) is limited to avoid complete discharges.

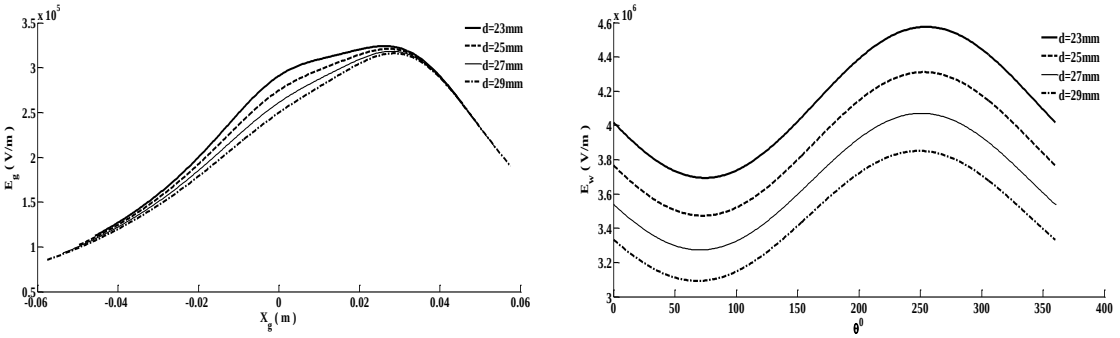

(a) on the ground plate (b) at the ionized wire

Figure 7. Variation of electrostatic field
(v=10kV, $2R_a$=14mm, $2R_w$=0.5mm, $2R_c$=25mm, h=20mm, x=25mm, y=25mm)

The influence of changing the horizontal distance (x) of the limiting cylinder on the profile of the electrostatic field on the ground surface is illustrated in Figure 8(a). It was recognized that the field is higher in the zone where the limiting cylinder is located. The maximum field on the ground increases as the limiting cylinder gets closer to the ionized wire. The maximum field decreases by 0.61%, 1.53 %, 2.42%, 3.28% when the limiting cylinder moves from x=15mm to 20, 25, 30and 35mm respectively. Obviously, as x increases, the influence of it becomes less significant. While slightly lowering the peak value by moving the limiting cylinder horizontally, it shifts the position of the peak on the ground surface.

Figure 8(b) presents the effect of moving the limiting cylinder horizontally on the profile of the electrostatic field at the ionized wire. The field at the ionized wire decreases as the limiting cylinder gets closer to the wire increasing the field on the ground. So, the field upon the ionized wire can be controlled by positioning the limiting cylinder keeping the ionized wire in its position. The maximum electric field at the wire is decreased by 2.27%, 5.09%, 8.61%, 13.12% when the limiting cylinder position is changed from x=35 to 30, 25, 20 and 15 mm respectively. The non-uniformity around the wire increases as the limiting cylinder gets closer to the wire. The variation between E_{max} and E_{min} is 17.87%, 18.52%, 19.44%, 20.79%, 22.96% at x= 35, 30, 25, 20 and 15 mm respectively. It must be noted that the angle at which the peak field occurs on the wire increases as the limiting cylinder gets far away from the wire.

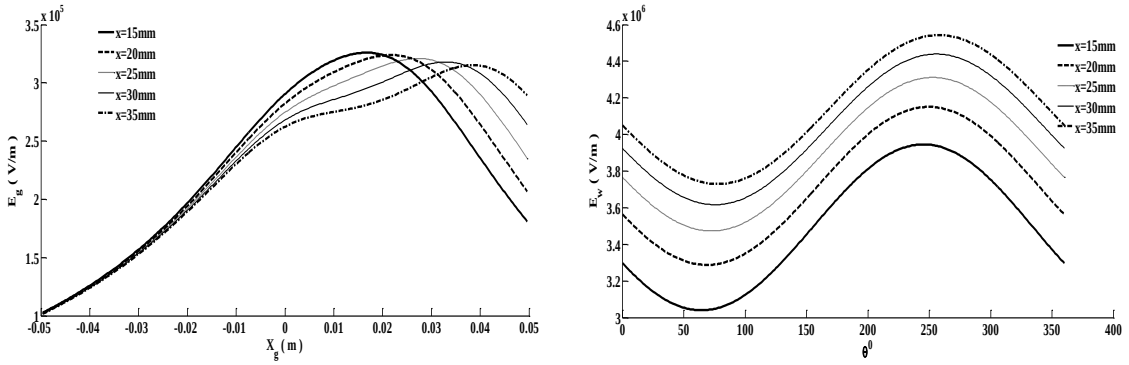

(a) on the ground plate (b) at the ionized wire

Figure 8. Variation of electrostatic field
(V=10kV, $2R_a$=14mm, $2R_w$=0.5mm, $2R_c$=25mm, h=20mm, d=25mm, y=25mm)

Figure 9(a) describes the variation of the vertical distance (y) of the limiting cylinder on the profile of the electrostatic field on the ground. It was showed that as the limiting cylinder gets closer to the ground plate, the field increases on the ground decreasing the field around the ionized wire. The maximum field increases by 7.92%, 15.47%, and 24.97% when the limiting cylinder differs from y=30 mm to 27, 25 and 23 mm respectively. Also, the peak on the ground surface is shifted to the right.

The influence of moving the limiting cylinder vertically parallel to the ionized wire on the profile of the electrostatic field on the ionized wire is demonstrated in Figure 9(b). The field on the ionized wire decreases as the limiting cylinder gets closer to the ground which justifies the fact of increasing the field upon the ground plate as the limiting cylinder gets closer to the ground plate. The maximum electric field on the wire is decreased by 1.8%, 2.99%, and 4.11% when the limiting cylinder position is changed from y=30 to 27, 25, and 23 mm respectively. The non-uniformity around the wire increases as the limiting cylinder gets closer to the ground. The difference between E_{max} and E_{min} is 19.64%, 19.44%, 19.22%, and 18.83% at y= 23, 25, 27 and 30 mm respectively.

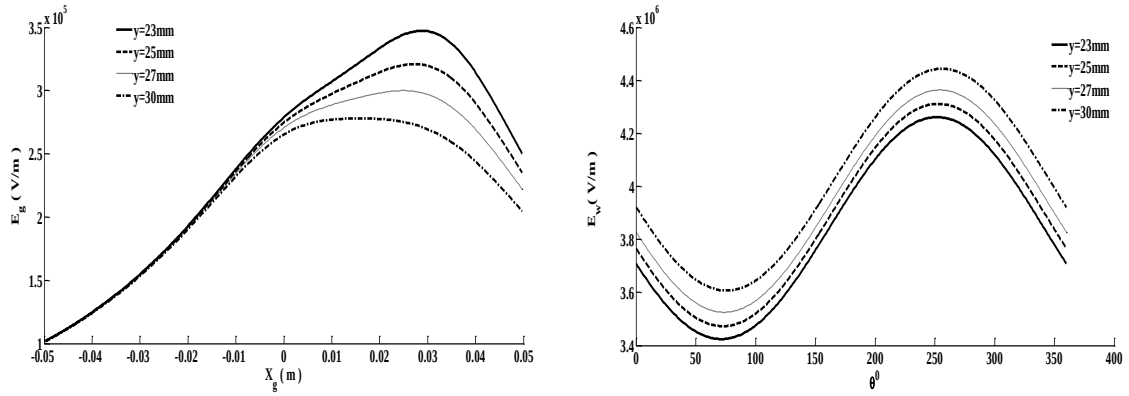

(a) on the ground plate (b) at the ionized wire

Figure 9. Variation of electrostatic field
(V=10kV, $2R_a$=14mm, $2R_w$=0.5mm, $2R_c$=25mm, h=20mm, d=25mm, x=25mm)

The measured corona onset voltage is compared with numerically computed onset voltage. If E_{on} is the electric field at onset computed by peek's formula then the corresponding corona onset voltage V_o is computed using V_o=V (E_{on} / E), where V is the voltage which produce an electric field of magnitude E at the surface of the wire and computed using the GA-CSM

algorithm [8, 18]. The distance between the ionized wire and the upper cylinder, h, is kept constant as well as the height of the ionized wire above the ground plate, d.

The measured and calculated values of the corona onset voltage for different ionized wire diameters of the ionized wire at different positions of the limiting cylinder along the x-axis at distance 25mm from the ground plate, y=25mm, as well as in the absence of the auxiliary cylinder (dual electrode system) are illustrated in Figure 10. The calculated onset voltage values are well agreed with those measured experimentally. The results shows that the corona onset voltage increases with increasing the ionized wire diameter. The addition of the limiting cylinder affects the corona onset voltage of the ionized wire. The corona onset voltage of the wire increased by 34.6%, 38.7%,40.25%,27.1% and 26.1% for wire diameters 0.25,0.4,0.5,0.8 and 1 mm respectively when the limiting cylinder is inserted to the dual electrode system at x=15mm from the ionized wire. The results confirms that as auxiliary cylinder gets closer to the ionized wire the corona onset voltage increases and vice versa.

Also, the effectiveness of changing the position of the auxiliary cylinder along the y-axis has been studied and measured experimentally keeping the limiting cylinder at fixed horizontal distance, x=15mm, from the ionized wire, Figure 11. The corona onset voltage of the wire increases by 38.5%,43.3%,45.6%,30.9% and30.4 % for wire diameters 0.25,0.4,0.5,0.8 and 1 mm respectively when the limiting cylinder is inserted to the dual electrode system at y=22mm from the ionized wire.

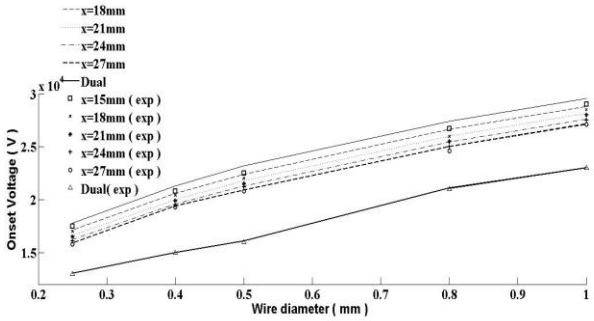

Figure 10. Measured and calculated corona onset voltage of ionized wire versus the wire diameter for different auxiliary cylinder position along x-axis (y=25mm, $2R_a$=14mm, $2R_c$=25mm, h=20mm, d=25mm)

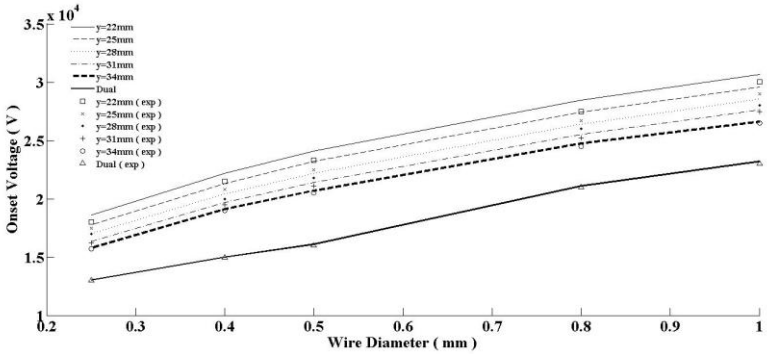

Figure 11. Measured and calculated corona onset voltage of ionized wire versus the wire diameter for different auxiliary cylinder position along y-axis (x=15mm, $2R_a$=14mm, $2R_c$=25mm, h=20mm, d=25mm)

5. Conclusion

The paper presents the computations and measurements of the various corona characteristics of a new electrode system intended for efficient charging of filtration media. The system incorporates an adjustable auxiliary cylinder, moving through the gap along both x-y axes, into the dual electrode configuration to increase its versatility and to provide reliability into controlling the field not only on the ionized wire surface but also along the ground surface. The arrangement offers symmetry, flexibility, high efficiency, and ease of operation in the filtration

media. Dependence of spatial distributions of the electric field on the ionized wire surface and along the ground surface on the system's geometrical parameters is examined and established. Detailed assessment of the role played by the auxiliary cylinder movement is presented and discussed. The effectiveness of the limiting cylinder movement in the two -dimensional on the corona onset voltage of the ionized wire is demonstrated. The configuration offers several advantages when compared with other designs as the use of the auxiliary cylinder leads to an increase of the electric field along the ground surface during the charging process of filtration media. Also, the electric field around the ionized wire is reduced with the presence of the auxiliary cylinder which allows extra blocking for the electric charges produced by corona discharges from dissipating to other ground equipment. The influence of changing the radius of the auxiliary cylinder and its location between the ionized wire and the limiting cylinder upon the ionized wire surface and along the ground surface is studied. The numerical onset voltage values agreed satisfactorily with those measured experimentally.

References

[1] Filters and Filtration Handbook. 6th Edition. Trevor Sparks and George chase. 2015.
[2] Plopeanu M, Notingher P, Dumitran L, B Tabti B, A Antoniu A, Dascalescu L. Surface Potential Decay Characterization of Non-woven Electret Filter Media. *IEEE Transactions on Dielectrics and Electrical Insulation*. 2011; 18(5): 1393-1400.
[3] Billington N. Air filtration. *Journal of the Institution of Heating and Ventilation Engineers*. 1947; 14: 46-95.
[4] Hassler J. Active Carbon - The Modern Purifier. New York: West Virginia Pulp and Paper Company. 1941.
[5] Marsh H, Rodriguez F. Activated Carbon. UK: Oxford. 2006: 14-16.
[6] Butonoi T, Gagiu G, Bilici M, Samuila A, Neamtu V, Morar R, Dascalescu L, Iuga A. *Electric and Electronic Equipment of a Research – Oriented Electrostatic Separator.* 12th International Conference and Optimization of Electrical and Electronic Equipment, OPTIM. 2010: 639-645.
[7] Starr E. High Voltage D.C. Point Discharges. *IEEE Transactions of the American Institute of Electrical Engineers*. 1941; 60(6): 356-362.
[8] Rafiroiu D, Morar R, Atten P, Dascalescu L. Premises for the Mathematical Modeling of the Combined Corona – Electrostatic Field of Roll-type Separators. *IEEE Transactions on Industry Applications*. 2000; 36(5); 1260-1266.
[9] Dumitran L, Badicu L, Plopeanu M Dascalescu L. Efficiency of Dual Wire –Cylinder Electrodes Used in Electrostatic Separators. *Revue Roumain des Sciences Techniques*. 2010; 55(2): 171-180.
[10] Abouelsaad M, Abouelatta M, Salama A. Experimental and numerical investigations of the corona characteristics of a new Tri-electrode system for electrostatic separation processes. *European Physical Journal Applied Physics*. 2014; 67(3): 1-11.
[11] Plopeanu M, Dumitran L, Noţingher P, Vihacencu M, Dascalescu L. Improvement of electric charging efficiency of the filtration media. *Journal of Electrostatics*. 2013; 75(4).
[12] Peek F. Ionisation Phenomena in High Voltage Engineering. New York: McGraw-Hill. 1929.
[13] Abouelsaad M, Abouelatta M, Salama A. Genetic algorithm-optimised charge simulation method for electric field modelling of plate-type electrostatic separators. *Science, Measurement & Technology IET*. 2013; 7(1): 1-7.
[14] Goldberg D. Genetic algorithms in search, optimization, and machine learning. Addison-Wesley. 1989.
[15] Sivanandam S, Deepa S. Introduction to genetic algorithms. Berlin: Springer. 2008.
[16] Haupt R, Werner D. Genetic algorithms in electromagnetic. New Jersey: John Wiley &Sons. 2007.
[17] Arora R, Halder P. *Investigation of the inception of streamer corona in SF6 gas.* 12th International Symposium on High Voltage Engineering. 2001; 4(25).
[18] Rafiroiu D, Suarasan I, Morar, Atten R, Dascalescu L. Corona inception in typical electrode configurations for electrostatic processes applications. *IEEE Transactions on Industry Applications*. 2001; 37(3): 766-771.